

Charles University

Faculty of Science

Study program: Special Chemical and Biological Programmes

Branch of study: Molecular Biology and Biochemistry of Organisms



Markéta Pelantová

Genetically encoded biosensors of cellular tension and their use in cellular biology

Geneticky kódované biosenzory buněčné tenze a jejich využití v buněčné biologii

Bachelor's thesis

Supervisor: doc. RNDr. Daniel Rösel, Ph.D.

Prague, 2019

Prohlášení:

Prohlašuji, že jsem závěrečnou práci zpracovala samostatně a že jsem uvedla všechny použité informační zdroje a literaturu. Tato práce ani její podstatná část nebyla předložena k získání jiného nebo stejného akademického titulu.

V Praze, 9.5.2019

Podpis

Acknowledgments

My huge thanks belong to my supervisor doc. RNDr. Daniel Rösel, Ph.D. for his endless patience, help and supervision. I would also like to thank my colleague Aneta and all my friends who helped me during writing of my thesis. Last, I wish to thank my family for supporting me throughout my whole studies.

Abstract and key words

Mechanical forces have great impact on the life of cells. They influence cell proliferation, migration or differentiation and defects in cellular mechanosensing were reported to be the cause of various diseases, such as deafness, atherosclerosis or cancer. However, mechanisms of mechanical sensing are not thoroughly examined and not many tools for doing such research are available. Genetically encoded FRET-based biosensors are one of the existing methods for studying transfer of mechanical signal in cells. It is a non-invasive method allowing to observe changes in mechanical tension across proteins in living cells. In this thesis, different types of existing genetically encoded FRET-based tension biosensors are introduced together with the process of their development and knowledge gained by their use in research.

Key words: mechanical force, mechanosensing, FRET, tension sensor, biosensor development

Abstrakt a klíčová slova

Mechanické síly mají velký vliv na celý život buněk. Ovlivňují buněčnou proliferaci, migraci či diferenciaci a chyby v buněčném vnímání mechanických sil se ukazují být jednou z příčin různých chorob jako je např. hluchota, ateroskleróza či rakovina. Mechanismy, kterými buňky mechanické síly vnímají, jsou nicméně ještě velmi málo probádány a chybějí nástroje, kterými by je bylo možné zkoumat. Geneticky kódované tenzní biosenzory využívající pro detekci tenze FRET jsou jednou ze současně používaných metod pro studium přenosu mechanického signálu v buňce. Jedná se o neinvazivní metodu, jejíž pomocí je možné v živých buňkách sledovat změny v mechanickém napětí na různých proteinech. V tomto textu jsou představeny různé typy existujících geneticky kódovaných tenzních biosenzorů využívajících FRET, proces jejich vytváření a objevy díky nim získané.

Klíčová slova: mechanická síla, mechanosenzitivita, FRET, tenzní senzor, příprava biosenzoru

List of abbreviations

aa	amino acid
ABS	Actin binding site
BDM	2,3-butanedione monoxime; inhibitor of actomyosin contractility
Cad	Cadherin
CS	Control sensor
DP	Desmoplakin
DSG	Desmoglein
E-cadherin	Epithelial cadherin
EcadTSMMod	E-cadherin tension sensor
EcadTSMMod Δ cyto	E-cadherin tension sensor control lacking the β -catenin binding domain
ECM	Extracellular matrix
FA	Focal adhesion
FL	Ferredoxin-like
FLIM	Fluorescence Lifetime Imaging
FRET	Förester resonance energy transfer
GFP	Green fluorescence protein
HP	headpiece peptide
HP35	35 aa long headpiece peptide
HP35st	35 aa long stable mutant of headpiece peptide
ICS	Cadherin-type sequence, also catenins-binding site; plakoglobin-binding site in desmoglein
KMSS	Zero-force control of the MSS
K-Ras	Protein from Ras family, membrane-attached
Lyn	Tyrosin-kinase from the Src family
MDCK	Madin-Darby canine kidney cells
MEKs	Murine epidermal keratinocytes
MSS	Membrane tension sensor

opt-	Optimized
PECAM-1	Platelet and endothelial cell adhesion molecule 1
RGD	Integrin-recognition sequence (Arg-Gly-Asp)
ROCK	Rho-associated protein kinase
TL	Tailless, usually name of zero-force control lacking one of the binding domains of the examined protein
Tln	Talin
TS	Tension sensor
TSM	Tension sensing module
TSMo	Tension sensing module with silk peptide as flexible linker
VBS	Vinculin binding site
VE-cadherin	Vascular endothelial cadherin
Vh	Vinculin head domain
Vin	Vinculin
VinV	Venus-labeled vinculin
Vt	Vinculin tail domain

Contents

1 Introduction	1
2 Mechanotransduction	1
3 Fluorescence	2
4 Förster resonance energy transfer	3
5 Silk peptide-based FRET tension biosensors	5
5.1 Spider silk peptide	5
5.2 Tension sensing module	5
5.2.1 Tension sensing module development	5
5.2.2 TSMMod sensitivity depends on length of its elastic part	6
5.3 The vinculin tension sensor	8
5.4 E-cadherin tension sensor	10
5.5 PECAM-1 tension sensor	12
5.6 Desmoglein-2 tension sensor	13
5.7 Desmoplakin sensor	15
5.8 Membrane tension sensor	16
5.9 TSMMod-based talin tension sensor	18
6 Tension sensors with other tension modules	19
6.1 Talin tension sensor	19
6.2 Talin ferredoxin-like peptide-based sensor	21
7 Conclusion	23
8 Literature	24

1 Introduction

One of the many factors influencing the life of the cell is a mechanical force. A cell must be able to sense mechanical forces, transform them into the intracellular biochemical signals and appropriately react to them. Unfortunately, we still don't know a lot about the molecular mechanisms of these processes and there are not many tools to explore them. One of the existing methods are FRET-based biosensors.

Biosensors are tools commonly used in biological research for detection of specific agents or activity of molecules. Their important feature is the ability to emit a signal we can detect and measure – often light emitted by a fluorophore attached to the biosensor. In cell biology applications, biosensors can have different origins. Most of them are protein based, but DNA-based sensors have also been developed [1].

Genetically encoded biosensors are protein-based sensors composed of a fluorescent protein fused to a sensing module. The recombinant biosensor is then transfected and expressed in live cells. That way the cells produce the biosensor themselves without the need for its external introduction.

The goal of this work is to summarize the design, use, advantages and disadvantages of genetically encoded FRET-based biosensors of cellular tension at the cell-ECM (extracellular matrix) interface.

2 Mechanotransduction

Intracellular signalling is based on biochemical signals, therefore there has to be a mechanism by which cells transfer signal from the extracellular space into a intracellular biochemical signal and response. Mechanotransduction is the process of transfer and interpretation of mechanical force signals such as external or internal tension, pressure, gravity or sound waves into intracellular biochemical signalling. The force can origin outside of the cell, but also inside of it. Also, the transformation of the signal can be executed either on the interface of ECM and membrane or inside the cell, for instance at the connection between the cytoskeleton and the nuclei [2]. It is not surprising that one of the types of molecules participating in mechanotransduction at the interface with ECM are proteins involved in formation of cell-ECM adhesion structures, such as focal adhesions (FAs) [3]–[6]. Another

example of molecules directly participating in mechanotransduction are mechanically gated ion channels in hair-cells localized in the inner ear [7].

Defects in mechanotransduction were reported to be associated with various diseases such as deafness [8], atherosclerosis [9] or cancer [10], [11]. Therefore, research of mechanotransduction is crucial for better understanding of these diseases.

3 Fluorescence

Fluorescence is a phenomenon when a certain compound, generally called a fluorophore, emits light after accepting energy in the form of electromagnetic radiation. Upon accepting energy, electrons in the fluorophore are excited to a state with higher energy. This state is called the excited state. When the electron returns to its ground state, it emits energy in the form of a photon of lower energy than the originally absorbed photon. This difference between the energy of the absorbed and emitted photon is called Stokes shift and is a result of a phenomenon called vibrational relaxation [12], [13].

The fluorophores differ in their features. One of the features is the quantum yield, i.e. the emission efficiency. It's commonly defined as the ratio of total energy quantum (photons) that are used to excite the fluorophore and the photons that are productively absorbed (meaning their absorption has led to the emission of a photon) [14]–[17]. Another important feature describing the quality of the fluorophore is fluorescence lifetime, which expresses the time needed for the fluorophore to return to its energy ground state by emitting the photon.

The most known genetically encoded fluorophore is the Green fluorescence protein (GFP), originally isolated from jellyfish *Aequorea victoria* [18]. Its major excitation peak is at the wavelength of 396nm (UV light) and its emission peak is at 509nm. However, there is a wide range of protein fluorophores derived from GFP [19]–[21] by genetical modification that differ in their emission and excitation wavelengths and other features, e.g. their stability in different conditions or their ability to fold correctly [19], [20]. All of the fluorescent proteins described in this work are summarized in (Fig.1A).

	Excitation peak	Emission peak	Quantum Yield	Brightness
Wt GFP	395nm	509nm	0.79	19.75
ECFP	434nm	477nm	0.4	13.0
mTFP	462nm	492nm	0.85	55.4
EGFP	488nm	507nm	0.6	33.54
Clover	505nm	515nm	0.76	84.36
Venus	515nm	528nm	0.57	52.55
mEYFP	515nm	528nm	0.62	48.98
YPet	517nm	530nm	0.77	80.08
tagRFP	555nm	584nm	0.48	48.0
mRuby2	559nm	600nm	0.38	42.94
mCherry	587nm	610nm	0.22	15.84

Fig.1: A) Excitation and emission peaks of fluorophores used as FRET pairs in sensors described in this work. Excitation and emission peaks, quantum yield as well as brightness were taken from <https://www.fpbases.org/>. Colours match the wavelength.

4 Förster resonance energy transfer

Förster resonance energy transfer (FRET) is a phenomenon that has been described by German physical chemist Theodore Förster [22]. It occurs between two fluorophores usually called donor and acceptor, whereas the emission spectrum of the donor has to overlap with the excitation spectrum of the acceptor (Fig. 2). FRET describes the phenomenon when the excitation energy is transferred from the donor to the acceptor fluorophore, which in turn emits the light. Theodore Förster created the equation describing the transfer rate of FRET (k_t), where R_0 is Förster constant (the proximity and orientation of fluorophores, when the efficiency of FRET equals 50%), r is the actual proximity of fluorophores and τ_0 is the lifetime of the unperturbed donor [23].

$$k_t = \frac{1}{\tau_0} \left(\frac{R_0}{r} \right)^6$$

As evident from the equation, the biggest impact on FRET has the proximity factor (r) – FRET decreases with growing proximity by the power of six. Therefore, FRET can occur only when the fluorophores are in close proximity (1-10nm). This limit for effective distance of the fluorophores corresponds well to distances common in biological intra- and also intermolecular interaction, such as protein interaction or change in the conformation after enzyme activation. When the distance between the acceptor and the donor is larger, no energy transfer can be observed [23].

All of the compatible FRET pairs described in this work are summarized in (Fig.2C).

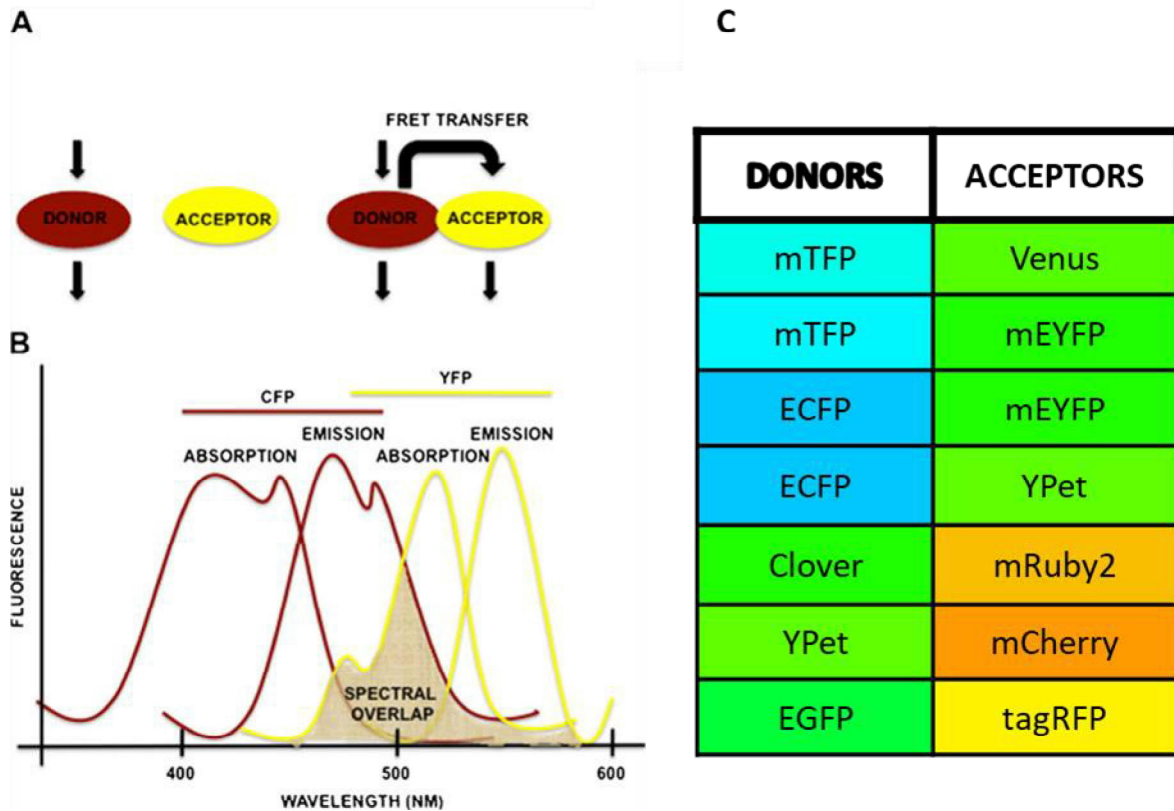


Fig.2: **A** FRET occurs only when the acceptor and the donor are in favourable proximity (1-10nm) **B** For a FRET pair to be compatible, the emission spectrum of the donor has to overlap with the excitation spectrum of the acceptor. The FRET pair CFP-YFP was used as a demonstration of a compatible FRET pair. Images **A** and **B** were taken from [24] and modified. **C** compatible GFP-based FRET pairs that are described in this work. Colours match the emission wavelength.

5 Silk peptide-based FRET tension biosensors

5.1 Spider silk peptide

One of the biological materials with the most interesting mechanical properties is the spider web formed by flagelliform silk protein. It is so unique it outclasses human-designed materials. It has to be strong and durable enough to capture relatively large insects. Its strength is comparable with steel, but unlike steel, spider's silk is also extremely elastic and has the ability to stretch 500-1000% [25]. It is also quite resilient and can be stretched repeatedly. Its elasticity is directly influenced by humidity – spider silk is covered in hydroscopic gluey coating and it maintains its elasticity when being wet and in its natural state. When dry, it's elasticity drops rapidly [26].

Spider silk also seems to have the ability to heal itself – when being stretched, there are rupture events corresponding to breaking of bonds and exposing hidden parts of the silk protein. These events occur with slight differences when repeating the stretch and relaxation, suggesting that the silk protein refolds when relaxed and doesn't have just one exact submolecular structure. Also, when stretching the silk protein, over the range from a few pN to 500-800pN, the force changes are exponential, but reasons for the exponentiality of the force are subject of discussion. One of the existing models presumes an interconnection of silk springs creating a molecular network with exponential dependence of the force [27].

The flagelliform of the silk protein isolated from spiderweb consists mostly of the repetitive β -spiral sequences, giving the silk protein its elasticity, and non-repetitive spacer sequences responsible for the strength of the silk protein. The most frequent sequence in the silk protein is (GPGGX)_n, where X = A, Y or V (alanin, tyrosin or valin) [27]. This sequence was used to create the first FRET-based tension sensor [28].

5.2 Tension sensing module

5.2.1 Tension sensing module development

In 2010, Grashoff and co-workers published an article describing the development and use of a FRET-based biosensor measuring force across proteins [28]. The tension sensing part of the biosensor is derived from the flagelliform of the spider silk elastic repetitive domain GPGGA. The tension sensing module (TSMoD) of the biosensor is composed of a 40 amino acids long

elastic spring formed by eight GPFGA repetitive sequences, which is inserted between two fluorophores mTFP1 and Venus. The mTFP1 and Venus represents an effective FRET pair compatible with FRET imaging. The level of tension-dependent extension of the elastic spring within the TSMOD then can be monitored as a decrease in FRET between mTFP1 and Venus [28].

5.2.2 TSMOD sensitivity depends on length of its elastic part

For testing the range of force the TSMOD is able to sense, the already existing procedure of using optical tweezers for testing tension sensor [28] was used, only in this case three peptides (named F25, F40 and F50) were constructed containing 25, 40 and 50 amino acids, respectively. These lengths match five, eight and ten repeats of the GPFGA sequence. Constructs were then flanked through DNA-oligonucleotides by 3'Cy3 and 3'Cy5 (Cy3 and Cy5 are fluorescent dyes, a compatible FRET pair). That way the distance between two dyes depended on the extension of the peptide. One end of the construct was then attached to a bead, the other end was tethered on to a polymer surface. Using optical tweezer, the bead was stabilized at one position, whereas the stage was repeatedly moved generating a tension across the peptide constructs. As expected, depending on growing force FRET values decreased as a result of extending distance between the donor (Cy3) and acceptor (Cy5). (Fig.3)

The FRET values between all three constructs differed – at the same applied force (1pN), F50 showed the lowest and F25 the highest FRET proving that the longer peptide extended more than the shorter one [29]. The results also demonstrated, that the silk-peptide spring's behaviour is linear despite the fact that in literature there is not much evidence indicating this – linear behaviour suggests a well-defined structure of the folded flagelliform which opposes other findings about the silk peptide [27], as previously described in the chapter 5.1 *Spider silk peptide*.

Results gained by experiments *in vitro* had to be tested in living cells as well. Therefore, the fluorescent proteins mTFP and Venus were attached to the F25, F40 and F50 constructs creating TSMODs of different lengths. Modules were then incorporated between two independent binding domains of vinculin – head (Vh) and tail (Vt) domain. That created the vinculin tension sensor (VinTS) of different lengths. As a control module, versions of the sensor lacking the tail domain (VinTL) were constructed (Fig.3B). These sensor variants were prepared using the previously described procedure, which was used to create the original

vinculin tension sensor [28] – described also in the chapter 5.3 *The vinculin tension sensor*. All constructs were then expressed in live cells plated on fibronectin-coated surface.

The localization of the VinTSs was unchanged from the normal vinculin – they all localized at focal adhesions and there they all displayed decreased FRET efficiency compared to their tailless opposites. FRET differed between the cells with VinTL modules, however, due to their missing tail domain, only because of different lengths of those constructs (F25, F40 and F50, see Fig.3C).

The F25 VinTS showed the lowest compliance (meaning it took the greatest force necessary to extend it) and the FRET changes were measurable in the range from 2 to 11pN. Lower forces than 2pN were not measurable with the same sensitivity due to the plateau of F25 sensor. Researchers carrying out the experiments offered two possible explanations for the plateau [29]. The first is that the tension constructs have a defined rod-like shape (which would also explain the linear behaviour described previously in this text) and when applying the force, the spring must first change its orientation in the direction of the applied force, which requires low-level force. Only after that the spring is ready to extend. The second explanation is that the small force enables more efficient alignment of the donor and acceptor, so the change of FRET due to the growing distance between them is in the beginning compensated by the the higher efficiency of FRET.

In range 2-6pN the sensitivity of all three lengths of the sensor acted almost the same despite the lower compliance of F25. Therefore from the three sensors, the F25 construct has the largest range of measurable force (2-11pN) [29]. However, because of sensitivity reasons, for the measuring of lower forces, use of a longer sensor would be more appropriate. For measuring higher forces, theoretically a shorter tension sensor could be constructed, but the plateau would presumably be larger as well.

The VinTS with F50 linker extended most with force, showing its highest compliance. For that reason, when the force was higher than 5pN, the sensor extended too much for FRET to be observed – it exceeded the measurable range 1-10nm. For smaller forces, the sensor was very sensitive – more sensitive than the F25 construct thanks to the absence of plateau.

Measuring of intracellular FRET across VinTS of all three lengths led to the same result, that tension across vinculin is about 2.4pN (Fig.3C).

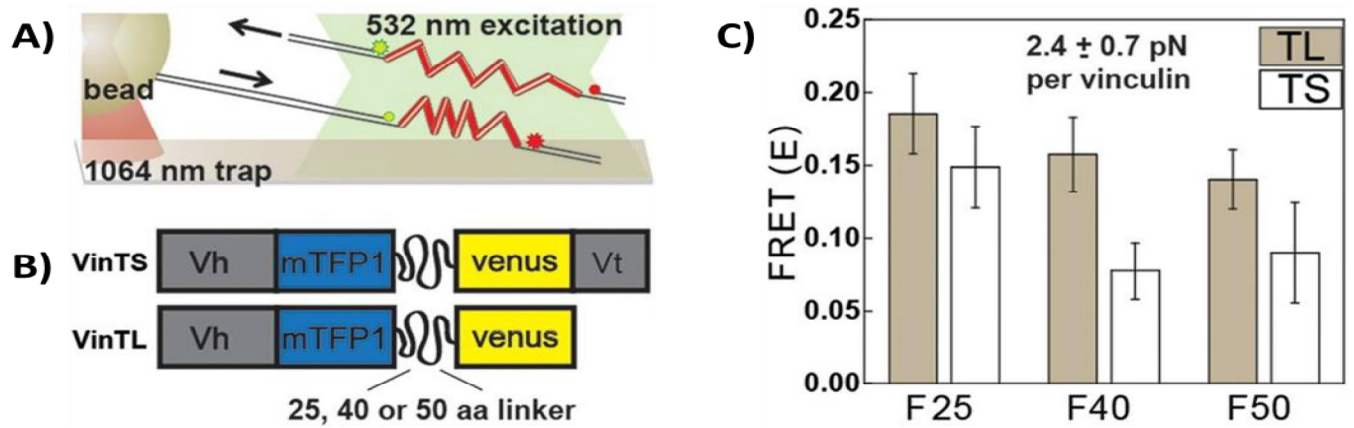


Fig.3: A) Model of measuring FRET dependence on extension of a linker by optical tweezers. B) Model of vinculin tension sensor and its tailless version. C) Intracellular FRET values of the tension sensor variants depend on the length of the flexible linker. TL stands for tailless version and TS for the tension sensor. Image was taken from [29] and modified.

There was also an attempt to improve TSMoD by using synthetic flexible linker (GGSGGS)_n. This synthetic version is less stiff than the silk peptide and *in vitro* displays better FRET efficiency. This wasn't observed in living cells, where the efficiency of both the original and synthetic linker was indistinguishable suggesting different behaviour of the sensors *in vitro* and *in vivo*. This indicates that *in vitro* calibration of sensors (later used in living cells) should be approached with caution [30].

5.3 The vinculin tension sensor

This sensor was the first silk-peptide-based tension sensor developed [28]. The TSMoD with 40aa linker was inserted in vinculin between its head (Vh) and tail (Vt) domain, creating a vinculin tension sensor (VinTS) [28] (Fig.4). The Vh domain has the ability to bind talin and by that recruit vinculin to focal adhesions (FAs). The Vt domain binds to F-actin and paxillin [31]. Besides VinTSs the vinculin tension sensor without the tail domain (VinTL) and vinculin labelled at the carboxy-terminal (VinV) were constructed (Fig.4). VinTL served as the zero-force control, whereas VinV was constructed for comparison to prove the normal localization of VinTS and VinTL in cells - both constructs (VinTS and VinTL) showed normal localization and full function in FAs.

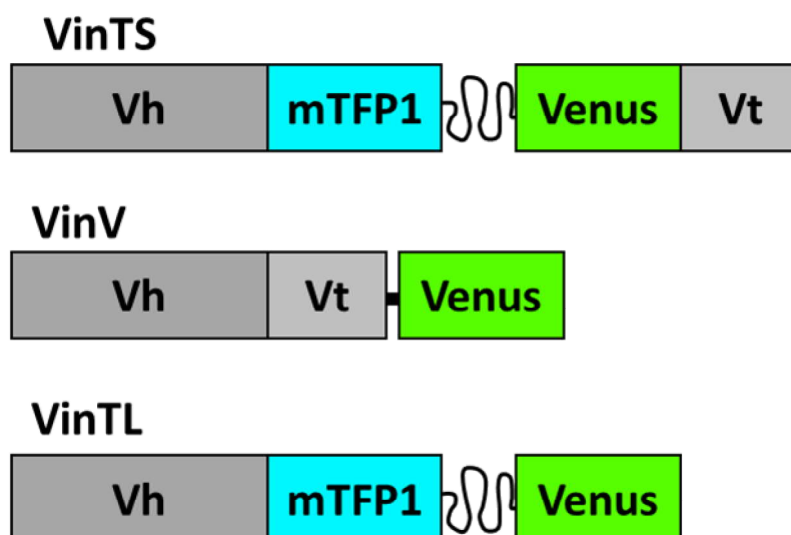


Fig.4: Model of Vin-TS and it controls VinV and VinTL (zero-force control). In VinTS the TSM domain was inserted between the head and tail domain. VinTL lacks the tail domain (binding F-actin and paxillin) and is therefore under no tension in cells. VinV is normal vinculin marked by Venus at its C-terminus. Image taken from [28] and modified.

Cells were seeded on two different substrates – fibronectin and poly-L-lysine. Poly-L-lysine helps to facilitate nonspecific cell attachment without integrin activation [32]. Fibronectin contains the so-called RGD sequence (Arg-Gly-Asp) enabling binding and activation of integrins and inducing formation of focal adhesions [33].

Fibronectin induced morphological changes and FAs formation, whereas on the poly-L-lysine coated plates cells stayed round. In cells on the poly-L-lysine plates, the values of FRET were high both for VinTS and VinTL – no force affected the cells. In cells on the fibronectin-coated plates, FRET values differed between VinTS and VinTL. VinTS showed lower FRET than VinTL suggesting increased mechanical force affecting the cells. Also, the lifetimes of VinTS were longer correspondingly with lower FRET [28].

Results of testing VinTS for sensitivity were that VinTS with a 40aa linker is most sensitive in range 1-6pN, which agrees with later findings [29] – also described in the chapter „Testing TSM domain sensitivity“ including the method used to test it.

Using FLIM-microscopy the force across vinculin in stabilized FAs was estimated at 2,5pN. Then, myosin-dependent contractility in cells was reduced by inhibiting the Rho-associated kinase and by RNA interference of myosinIIa resulting in a decrease of FAs size and an

increase in FRET comparable to the VinTL construct. Surprisingly, the vinculin sensor still localized at FAs in open conformation. This indicates, that the recruitment of vinculin and transmission of force are two separable processes regulated separately.

For measuring the force across vinculin in FAs the sensor was later optimized. The evaluation of the TSMods mechanical sensitivity showed that the construct with 9 repeats of the flexible linker has the best predicted sensitivity in range 1-6pN (range occurring in FAs across vinculin). Therefore, the sensor with nine repeats of the silk peptide sequence was chosen to create the optimized vinculin sensor (opt-VinTS). Moreover, instead of the original mTFP1-Venus FRET pair, the pair Clover/mRuby2 was used since it displays stronger FRET at the given Förster radius (for complete development of the opt-VinTS see the original article [30]). The opt-VinTS displayed much higher sensitivity and enabled to clearly visualize gradients of vinculin tension in FAs which is not easy to do when using the original VinTS [30].

Besides the regulation of FAs dynamics the vinculin tension sensor helped to reveal many other processes, such as the control mechanism of vinculin loading [30], the regulation of forces at cell-matrix adhesions in mesenchymal cells [34] or that the tension in FAs influences migration potential of tumour cells [35].

5.4 E-cadherin tension sensor

Cadherins are transmembrane proteins with two domains. The extracellular domains of cadherins interact with each other creating intercellular connections, whereas the intracellular domain recruits catenins which then interact with F-actin [36], [37].

To enlighten the role of cadherins in mechanotransduction the tension sensor was constructed [4]. The TSMOD (with mTFP and mEYFP as FRET pairs and the linker F40) was inserted into the intracellular part of E-cadherin between the catenin-binding and transmembrane domain, creating EcadTSMOD (Fig.5). This sensor, as well as control EcadTSMOD Δ cyto (lacking the β -catenin-binding site and therefore unable to recruit catenins), localized at the membrane and were recruited to cell-cell adhesions similarly to the endogenous E-cadherin. When expressed in cells without cadherin expression, the EcadTSMOD was also able to rescue the cell-cell adhesion. Due to that it is safe to say that E-cadherin with the tension sensing module stayed fully functional. The intermolecular FRET was found to be negligible.

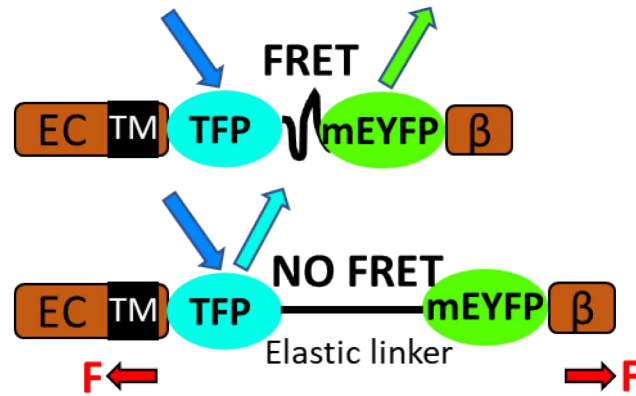


Fig.5: Model of EcadTSMOD. Sensor module is inserted between the transmembrane and β -catenin-binding domain. When force applied, flexible linker stretches which results in decrease of FRET. Image was taken from [4] and modified.

FRET was measured for EcadTSMOD and EcadTSMOD Δ cyto localized at cell-cell adhesions, EcadTSMOD and EcadTSMOD Δ cyto localized at the membrane without intercellular contact and for TSMOD expressed in cytoplasm. FRET of EcadTSMOD in cell-cell adhesion was significantly lower when compared to both TSMOD and EcadTSMOD Δ cyto. This indicates that molecular tension of E-cadherin in cell-cell adhesion depends on the β -catenin-binding domain. The FRET of EcadTSMOD outside cell-cell adhesion was higher than across EcadTSMOD in cell adhesions but still significantly lower than both free cytoplasmic TSMOD and EcadTSMOD Δ cyto suggesting, that even without intercellular connection E-cadherin is under small constitutive tension. (This result is however questionable, for in another study, where the researchers studied VE-cadherin, no significant constitutive tension across VE-cadherin outside of cell-cell junctions was to be observed [38].)

To test if the reason for tension across E-cadherin is due to the actomyosin activity, actin polymerization and myosin activity were inhibited by cytochalasin B and ML-7 respectively [39], [40]. Both treatments led to decrease in tension and therefore increase in FRET values for both the free-membrane and cell-cell adhesion EcadTSMODs.

Together, the results showed that actin-myosin contractility induces tension across membrane-bound E-cadherin, and that binding of β -catenin is necessary for this tension to appear. Moreover, E-cadherin recruited to cell-cell adhesions is under higher tension when compared to membrane-bound E-cadherin outside the adhesions [4].

In other study, the researchers used the E-cadherin sensor with Venus instead of mEYFP as the acceptor (CadTS) [41]. When examining migration of cell clusters in *Drosophila*, difference in tension between migrating cells was revealed – higher tension in the front of the migrating cluster than in the back indicating directional sensing of the cluster [41]. However, these results and CadTS itself were later challenged by a different study examining cell migration in *Drosophila* [42].

Another cadherin sensor was constructed using the same TSMoD as in vinculin sensor [28] for examining the effect of fluid shear stress on endothelial cells of the vascular – VE-cadherin sensor (VECadTS) [38]. In this study they used combination of two biosensors – VE-cadherin biosensor and PECAM-1 biosensor. Results gained from this study are presented in the chapter PECAM-1 sensor.

5.5 PECAM-1 tension sensor

In the vascular system the blood-flow influences the vascular morphology thanks to mechanotransduction [43]. Two of the proteins participating in this are VE-cadherin and PECAM-1. Inserting the TSMoD from the vinculin sensor [28] into PECAM-1, the sensor PECAM-TS was created [38] (Fig.6).

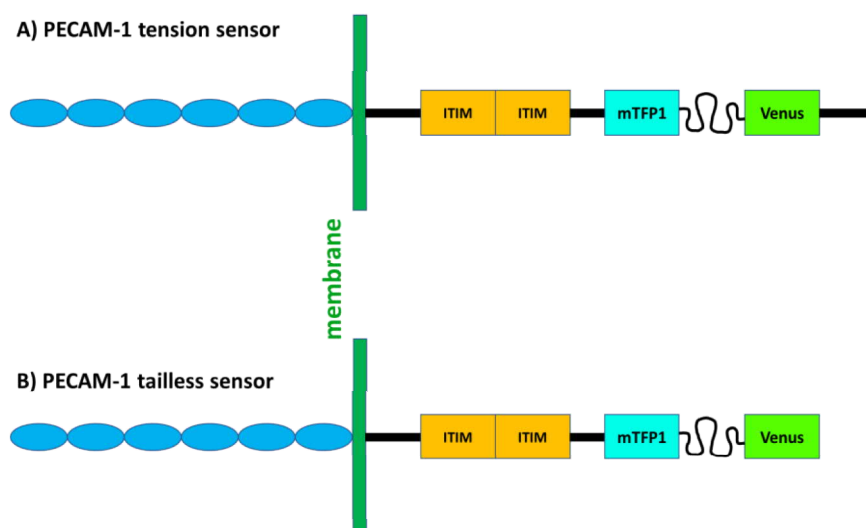


Fig.6: Model of PECAM-1 tension sensor and its tailless zero-force control. Tension module was inserted below immunoreceptor tyrosine-based inhibitory motif (ITIM) before exon 15. Image was adapted from [38] and modified.

The tension was measured across PECAM-1 and across VE-cadherin (using VECadTS described in the chapter 5.4 *E-cadherin tension sensor*) in endothelial cells and changes in FRET after application of fluid shear stress were examined. The results showed that flow induced about 25% drop in tension across VE-cadherin due to the weakening of cell-cell and cell-ECM forces, whereas tension across PECAM-1 increased. It was also proved that changes across PECAM-1 and VE-cadherin induced by flow are dependent on simultaneous presence of both proteins. Also, interaction between vimentin and PECAM-1 was induced by the fluid shear and this interaction was necessary for increase of tension across PECAM-1. The results together showed the relationship of VE-cadherin, PECAM-1 and vimentin [38].

5.6 Desmoglein-2 tension sensor

Desmoglein is transmembrane protein of the cadherin family existing in desmosomes (intercellular junctions e.g. of muscle, epidermal and epithelial cells). It is connected to intermediate filament through other proteins, such as plakoglobin or plakin protein family – for instance desmoplakin [44], [45] (desmoplakin's role in bearing mechanical force will be described in the following chapter). Pemphigus an autoimmunity disease is associated with this protein – the body creates antibodies against desmoglein and causes the separation of epidermal cells, which results in blisters on the skin [46].

The tension FRET-based biosensor was created to examine the role of desmoglein in cell-cell connection and its ability to bear force when the desmosome is subject to tensile loading.

The previously designed TSMoD [28] was inserted between the intercellular anchor and catenin-binding site (ICS, also cadherin-type sequence) which binds plakoglobin. (Fig.7).

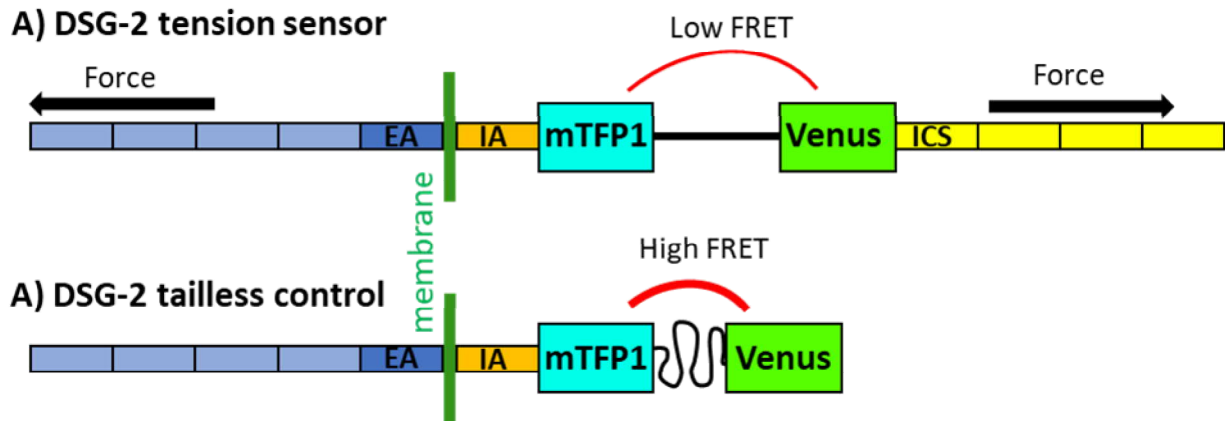


Fig.7: A) Localization of TSMod in DSG-2 tension sensor. TSMod was inserted between the intercellular anchor and catenin-binding site (ICS). EA stands for extracellular anchor. **B)** Zero-force tailless control lacking the ICS domain. Image was taken from [47] and modified.

After expressing the biosensor in cardiomyocytes and testing their functionality, the cells were exposed to mechanical force. However, it was impossible to measure FRET in actually beating cardiomyocytes (the cells moved too fast), therefore only the tonic contractions were induced by high concentration of K^+ and the relaxation by low concentration of K^+ in combination with 2,3-butanedione monoxime (BDM), which works as an actomyosin inhibitor and, therefore, relaxant.

Measurements in cardiomyocyte showed significant decrease of FRET in cells in the buffer with high concentration of K^+ (tonic contractions) compared to cells in the BDM buffer (relaxation). That indicates higher tension in contractile cells, although a small decrease was also visible in cells with the control sensor without the catenin-binding domain. That suggests that not all (but definitely most) of the tension across desmoglein-2 was a result of tensile loading.

[47]

Examination of FRET in desmosomes in resting (unstretched) epidermal and epithelial cells both showed that desmoglein-2 (and thus desmosomes themselves) is under a constitutive tension. The force across desmoglein-2 in resting cells (without applying any external force) was estimated at 1,5pN, which is comparable to E-cadherin [4].

Together the results proved, that desmoglein-2 in desmosomes is under constitutive tension in epithelial and epidermal cells, and that in cardiomyocytes the tension increases when the cells are being exposed to contractions.

5.7 Desmoplakin sensor

To study the role of desmosomes in mechanical loading another sensor was designed – a desmoplakin sensor [48]. Desmoplakin has N-terminal cadherin-binding and C-terminal intermediate filament binding domain, thus providing desmosomes with connection to intermediate filaments [49]. There are two split versions of this protein that are argued to have distinct function – desmoplakin I (DPI) and desmoplakin II (DPII) [50]. TSMOD [28] marked by FRET pairs mTFP1/mEYFP and YPet/mCherry (instead of mTFP1/Venus) was inserted in DPI and DPII, respectively (Fig.8). Final DPI tension sensor (DPI-TS) was then expressed in Madin-Darby canine kidney cells (MDCK) and DPII tension sensor (DPII-TS) in murine epidermal keratinocytes (MEKs).

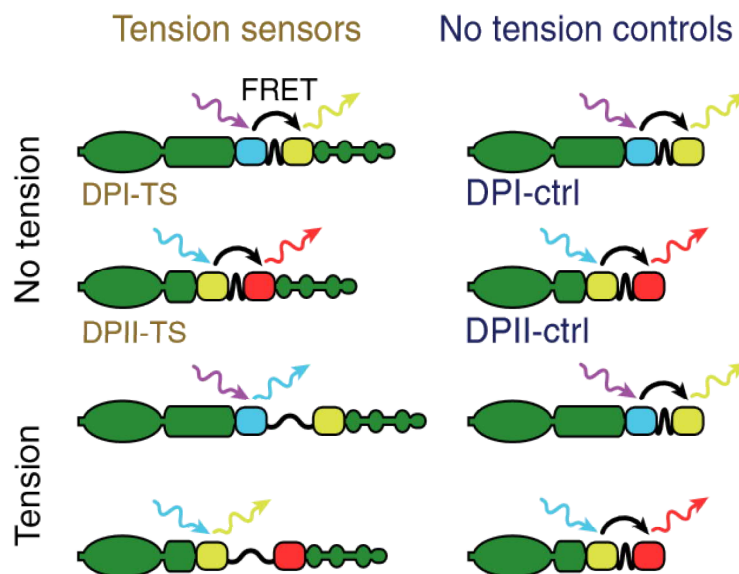


Fig.8: Desmoplakin tension sensors DPI-TS and DPII-TS with their zero-force controls lacking the keratin-binding domain. Image was taken from [48].

Measurements showed no differences in FRET depending on the confluence of cells. Also, in migrating cells, there were no changes to be observed. The actomyosin activity was inhibited

using cytochalasin-D (destabilizing actin) and inhibitor of Rho-associated kinase (inhibiting myosin function) to examine the effect of internal forces at desmoplakin. No difference was observed, not even after destroying the keratin network by okadaic acid.

This suggests that desmoplakin (and thus the desmosome) is under no tension in resting cells [48]. These results are in conflict with results gained by measuring tension across desmoglein [47]. Researchers offered a possible explanation – alternative connection of desmosomes to cytoskeleton than by desmoplakin, but to prove this, role of other desmosome-associated proteins needs to be thoroughly examined.

5.8 Membrane tension sensor

To examine dynamics of the cell membrane, a membrane-bound FRET-based tension sensor (MSS) was developed [51]. It differs from the other sensors described in this work, for this sensor isn't part of a naturally existing protein in the cell. It is rather an independent probe expressed in cells.

The MSS consists classically of the F40 flexible linker derived from silk peptide with donor and acceptor at the ends (ECFP and YPet). Besides this on both ends there are myristoylation and palmitoylation sequence from Lyn kinase (N-terminus) and prenylation signal from K-Ras (C-terminus) operating as anchor to lipid molecules in or out of the lipid raft in plasma membrane. With both sides of the sensor attached to the plasmatic membrane, this sensor is able to measure tension in the membrane. Control zero-force construct (KMSS) lacks the ability to bind with the N-terminal to the membrane – it is anchored to the membrane at one side only (Fig.9).

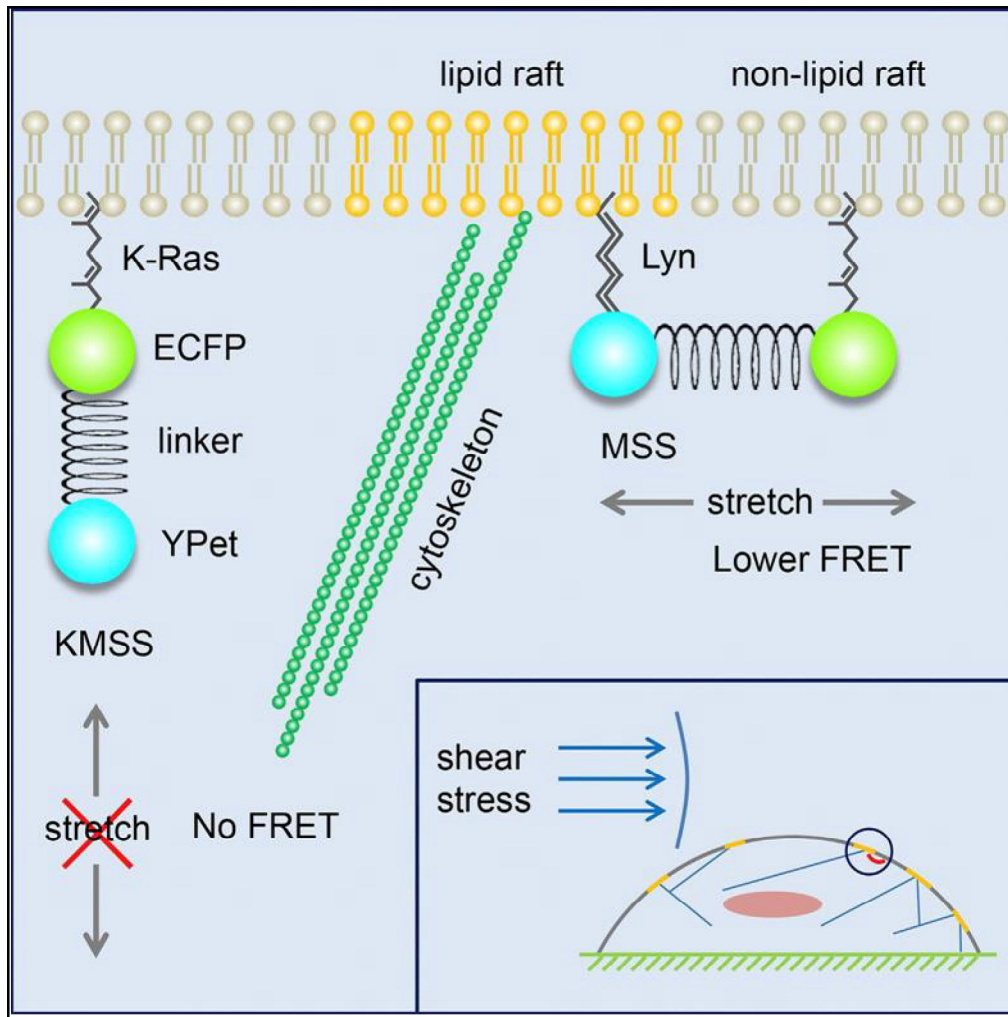


Fig.9: Schema of the MSS tension sensor. Flexible linker flanked by ECFP and YPet is anchored through Lyn and K-Ras sequence to the membrane. Shear stress induces stretching of the MSS resulting in lower FRET. Image was taken from [51].

The transfected HeLa cells were exposed to shear stress of three levels – 0,5, 2 and 4Pa. The FRET values changed, but surprisingly not linearly to the force applied – lowest FRET values were for 0,5 and 4Pa, higher for 2Pa. Shear stress therefore influences membrane tension, but not in a linear way. Another phenomenon observed was the apparent uneven distribution of tension – highest tension in the middle part of the dorsal membrane surface (with respect to the shear stress flow) and lowest in the front and back parts, which didn't change rapidly when the shear stress was applied [51].

Cells were also treated by cholesterol and benzoyl alcohol to increase or decrease the rigidity of the membrane, respectively, and then exposed to 2Pa shear stress. Results showed that, compared to control cells that weren't treated with either cholesterol or benzoyl alcohol,

enhanced fluidity of the membrane led to an increase of tension across the membrane and cholesterol enhanced rigidity resulted in lower tension.

Overall, the study shows usefulness of the MSS for examining mechanical properties of the plasmatic membrane.

5.9 TSMOD-based talin tension sensor

Talin is an intracellular protein linking integrins to actin [52], [53] and it undergoes tension itself. Talin has three F-actin binding sites (ABS) and many vinculin binding sites (VBS). When under tension, VBSs are revealed to vinculin, which can bind and then connect to actin by its own ABS [54]–[57]. For measuring tension across talin, the TSMOD [28] with EGFP/tagRFP FRET pair (instead of mTFP1/Venus) was inserted between the head and rod domain of talin creating talin tension sensor (talin-TS) [57]. Zero-force control talin-CS was constructed by inserting the same tension module with added linker (the linker prevents any influence at ABS3) at the C-terminal end of talin (Fig.10).

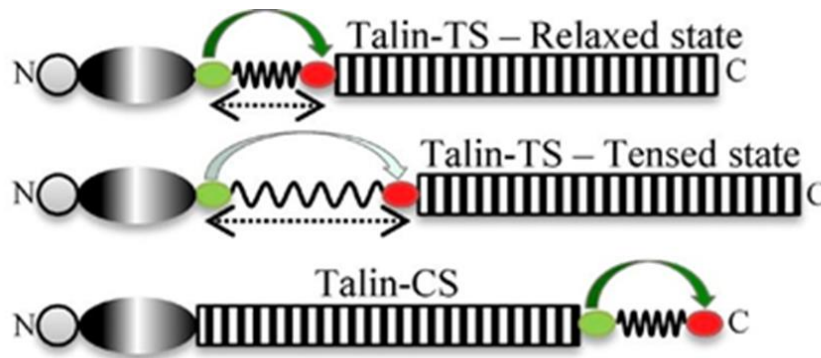


Fig.10: Model of talin-TS in tensed and relaxed state and its zero-force control talin-CS. Image was taken from [57] and modified.

At fibronectin-coated plates, cells expressing talin-TS displayed lower FRET in FAs than cells with talin-CS indicating tension across talin. To prove dependence of tension on actomyosin activity cells were treated with blebbistatin which inhibits the myosin activity by inhibiting the myosin ATPase activity [58]. Longer exposition to this inhibitor leads to disassembly of FAs [59]. Blebbistatin treatment indeed led to increase of FRET in talin-TS expressing cells, there was no change in talin-CS cells. Similarly, the induced increase in the

the myosin activity led to decrease of FRET in talin-TS cells (with no effect on the talin-CS cells) proving the requirement of myosin activity for tension across talin.

Also, measuring of FRET revealed differences between the peripheral (on the edge of cells) and central (near the nucleus) FAs – peripheral FAs displayed lower FRET than the central FAs, cells with the control construct displayed no such a difference. Expressing the talin-TS in vinculin-lacking cells didn't influence this difference indicating that the difference between peripheral and central FAs is vinculin-independent.

Talin stiffness-sensing was measured by seeding the cells on gels of different rigidity. Talin-TS displayed higher FRET at softer substrate compared to more rigid substrate, whereas talin-CS showed no stiffness-dependent difference. Also, tension across vinculin was measured using the Vin-TS, but this sensor displayed no stiffness-dependent changes in tension across vinculin. The results lead to conclusion, that vinculin (opposite talin) does not take part in rigidity sensing.

However, expressing talin-TS in cells lacking the vinculin expression revealed that vinculin contributes to tension across talin. Mutation of the talin ABSs and following measurements of FRET in talin-TS and talin-CS cells resulted in discovery that ABS3 is responsible for the differences in tension between peripheral and central FAs, but it is not necessary for force transmission, whereas ABS2 plays major part in this process [57].

6 Tension sensors with other tension modules

6.1 Talin tension sensor

Talin is a cytosolic protein, which has two isoforms – talin-1 and talin-2 that have slightly distinct functions [60]. It works as a linkage between integrins and actin [52]. The TSMods [28] sensitivity range is only 1-6pN, but force across integrins can be higher [61], which suggest the possibility of tension across talin also being higher - for measuring tension across talin different FRET-based biosensor was developed [62].

Instead of the silk peptide, villin headpiece peptide of the length 35aa (HP35) and its more stable mutant (HP35st) were used as linkers in the tension module. HP35 is a protein, that can be in three states of folding: folded, half-folded/half-unfolded and unfolded depending on

force across it. There is a transition of the folding/unfolding and at certain force this transition is equilibrium – at about 7pN for the HP35 and 10pN for the HP35st [63]. Therefore, by examining the folding state of HP35st it is possible to measure higher forces than by HP35.

FRET pair YPet and mCherry was attached to HP35 and HP35st creating HP35-TS and HP35st-TS [62], respectively (Fig.11). Optical tweezers were used for single-molecule calibration – both sensors showed fast recovery of their original folded conformation after releasing force, the equilibrium transition was at 7,4pN for H35-TS and 10,6pN for HP35st-TS. Both results showed that physical properties of the HP35(st) in sensor was unaffected by present fluorophores. Based on the measurement the highest sensitivity for both sensors was estimated: 6-8pN for HP35-TS and 9-11pN for HP35st.

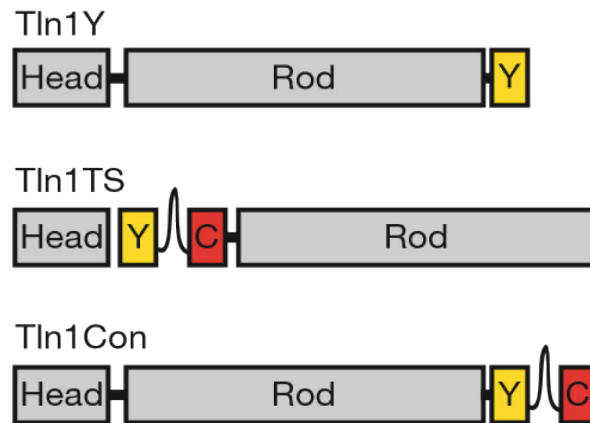


Fig.11: Model of talin tension sensor and its controls. As a linker either HP35 or HP35st is used. In tension sensor the tension module was inserted between the head and rod domain, in control it was inserted at the C-terminus. Y stands for YPet and C stands for mCherry. Image was taken from [62] and modified.

The tension sensor HP35 was inserted in a region between the head and rod domain of talin-1 (Tln1TS). As controls, talin-1 was C-terminally tagged by H35-TS (Tln1Con, zero-force control), YPet (control of functionality of talin-1 and intermolecular FRET) and mCherry (control of intermolecular FRET). All constructs showed full functionality proved by rescue of cells lacking talin-1 and talin-2 expression, physiological localization and negligible intermolecular FRET was observed measuring FRET in cells coexpressing the YPet-tagged and mCherry-tagged talin-1.

The tension across talin is myosin-dependent and to prove it, ROCK inhibitor Y-27632 was used to inhibit myosin activity with expected results – no effect in control cells and increased FRET efficiency in Tln1TS cells.

The relationship between talin-1 and vinculin was examined by expressing Tln1TS in cells with and without vinculin expression, since talin rod domain has 11 vinculin-binding sites. In vinculin-deficient cells measured FRET was higher than in vinculin-expressing cells indicating that tension across talin is vinculin dependent. After treating the vinculin-deficient cells with ROCK inhibitor Y-27632 the FRET was even higher suggesting that low-force tension across talin is not a result of interaction between talin-1 and vinculin, but only talin-1 and actin, whereas vinculin is necessary only for higher-force tension.

Measuring FRET in various talin-1 versions with deleted actin-binding and vinculin-binding sites showed that for binding of vinculin to talin-1 (and that way increase in tension across talin-1), preceding interaction of cytoskeleton and vinculin is needed.

The HP35-TS was also inserted in talin-2 and the differences in bearing force between talin-1 and talin-2 were examined. Results proved differences between talin isoforms and that those differences are rod domains R1-R3 dependent.

The HP protein-based talin sensor was later used in further studies. It helped to reveal the relation between actin, vinculin and talin in focal adhesions [64]; in combination with TSMMod-based talin sensor (which is not described in this work) it helped to examine the role of talin in developing muscle attachments in *Drosophila* [65].

6.2 Talin ferredoxin-like peptide-based sensor

Silk peptide-based TSMMod was proved to be a suitable sensor to measure tension, but the spring-like response (gradual extension of sensor depending on force) enables merely an average value of tension across the type of molecule being examined and it would be rather difficult to determine the percentage of molecules actively mechanically responding.

To overcome this problem with linear extension of TSMMod, a new ferredoxin-like peptide-based tension module (FL-TSM) was developed [66]. Its folding state changes very quickly depending on applied force and this folding transition isn't gradual, therefore it displays near-

digital force response, which enables to determine the portion of molecules actively mechanically engaged [66].

Single-molecule calibration showed FL-TSM to be sensitive in range 3-5pN. FL-TSM stayed folded up to 3pN, whereas 5pN force induced fast unfolding of the protein with equilibrium of folded/unfolded form at 4pN. The unfolding was reversible - the FL-TSM returned to its original form very quickly after releasing the force [66]. TSMoD with its spring-like form does not experience this unfolding event [28] – therefore force-responses of FL-TSM and TSMoD are very different. FL-TSM also displayed better zero-force FRET efficiency enabling more sensitive measurements.

The FL-TSM was inserted in talin-1 at two different places – after aa 447 and aa 1973 (Fig.12). In combination with TSMoD-based and HP35-based talin sensors talin behaviour was thoroughly examined. Beside confirming previously described talin properties as dependence on vinculin and rigidity sensing [62], [64], this study also showed intramolecular force gradient in talin-1 – C-terminal parts of talin experiencing lower forces than N-terminal regions, where measured force was more than 7pN.

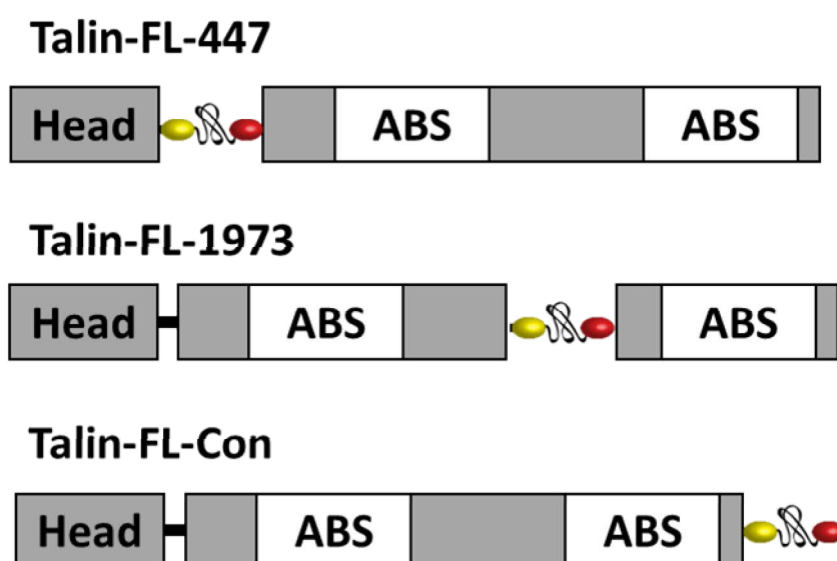


Fig.12: Model of talin FL sensor. FL-TSM module was inserted after aa 447 (Talin-FL-447) and after aa 1973 (Talin-FL-1973). Control has FL-TSM at C-terminus (Talin-FL-Con. Image was taken from [66] and modified.

In summary, the results proved high sensitivity of FL-TSM in the range 3-5pN, as well as its usefulness when estimating the ratio of mechanically active molecules [66].

7 Conclusion

FRET-based tension sensors are a unique non-invasive method for measuring very low forces that occur across molecules experiencing tension. Sensors described in this work are based on the same principle – force-dependent change of distance between two fluorophores resulting in measurable changes in FRET efficiency. Change of the distance can be reached by unfolding of a protein, as in FL-TSM and HP35-TS,[65], [66][65], [66] or (in case of most existing sensors) by extension of a flexible protein structure, as in TSMMod. In the first case, the range of measurable forces is dependent on the stability of the protein's folded form and on how sharp the transition between folding states is. In the second, case the sensitivity is directly influenced by length and stiffness of the flexible linker.

The sensitivity ranges of existing FRET tension modules together enable us to accurately measure forces in range of 1-12pN which is sufficient for most protein-protein interactions. Also, the sensors appear not to be limited by cell-types or organisms making it possible to use the same sensor in various models and to compare them.

However, analysis of the results gained by FRET-based tension sensors should be approached with caution, since the process of preparing appropriate controls, testing and calibrating the method is complicated and should not be underestimated.

Overall, FRET-based biosensors offer us better understanding of mechanical sensing in cells and show great promise for their future use in this area.

8 Literature

* ... references marked by this symbol are from a review

- [1] C. Buranachai, P. Thavarungkul, and P. Kanatharana, "A Novel Reconfigurable Optical Biosensor Based on DNA Aptamers and a DNA Molecular Beacon," *J. Fluoresc.*, vol. 22, no. 6, pp. 1617–1625, Nov. 2012.
- [2] M. L. Lombardi, D. E. Jaalouk, C. M. Shanahan, B. Burke, K. J. Roux, and J. Lammerding, "The interaction between nesprins and sun proteins at the nuclear envelope is critical for force transmission between the nucleus and cytoskeleton," *J. Biol. Chem.*, vol. 286, no. 30, pp. 26743–26753, 2011.
- [3] M. A. Schwartz, "Integrins and Extracellular Matrix in Mechanotransduction," *Cold Spring Harb. Perspect. Biol.*, vol. 2, no. 12, pp. a005066–a005066, Dec. 2010.
- [4] N. Borghi *et al.*, "E-cadherin is under constitutive actomyosin-generated tension that is increased at cell-cell contacts upon externally applied stretch," *Proc. Natl. Acad. Sci.*, vol. 109, no. 31, pp. 12568–12573, Jul. 2012.
- *[5] M. A. Schwartz and D. W. DeSimone, "Cell adhesion receptors in mechanotransduction," *Current Opinion in Cell Biology*, vol. 20, no. 5, pp. 551–556, Oct-2008.
- *[6] D. E. Ingber, "TENSEGRITY: THE ARCHITECTURAL BASIS OF CELLULAR MECHANOTRANSDUCTION," *Annual Review of Physiology*, vol. 59, no. 1, pp. 575–599, Oct-1997.
- *[7] D. Ó Maoiléidigh and A. J. Ricci, "A Bundle of Mechanisms: Inner-Ear Hair-Cell Mechanotransduction," *Trends in Neurosciences*, vol. 42, no. 3, Elsevier Ltd, pp. 221–236, Mar-2019.
- *[8] M. A. Vollrath, K. Y. Kwan, and D. P. Corey, "The Micromachinery of Mechanotransduction in Hair Cells," *Annu. Rev. Neurosci.*, vol. 30, no. 1, pp. 339–365, Jul. 2007.
- [9] C. Cheng *et al.*, "Atherosclerotic lesion size and vulnerability are determined by patterns of fluid shear stress," *Circulation*, vol. 113, no. 23, pp. 2744–2753, Jun. 2006.
- [10] S. Liang, M. J. Slattery, D. Wagner, S. I. Simon, and C. Dong, "Hydrodynamic shear rate regulates melanoma-leukocyte aggregation, melanoma adhesion to the endothelium, and subsequent extravasation," *Ann. Biomed. Eng.*, vol. 36, no. 4, pp. 661–671, Apr. 2008.
- *[11] D. E. Jaalouk and J. Lammerding, "Mechanotransduction gone awry," *Nature Reviews Molecular Cell Biology*, vol. 10, no. 1, pp. 63–73, Jan-2009.
- [12] H. Fujisaki and J. E. Straub, "Vibrational energy relaxation in proteins," *Proc. Natl. Acad. Sci.*, vol. 102, no. 19, pp. 6726–6731, May 2005.
- [13] P. Abbyad, W. Childs, X. Shi, and S. G. Boxer, "Dynamic Stokes shift in green fluorescent protein variants," *Proc. Natl. Acad. Sci.*, vol. 104, no. 51, pp. 20189–20194, Dec. 2007.
- [14] A. D. Kummer *et al.*, "Dramatic reduction in fluorescence quantum yield in mutants of Green Fluorescent Protein due to fast internal conversion," *Chem. Phys.*, vol. 237, no. 1–2, pp. 183–193, Oct. 1998.
- [15] K. P. Wall, R. Dillon, and M. K. Knowles, "Fluorescence quantum yield measurements of fluorescent proteins: A laboratory experiment for a biochemistry or molecular biophysics laboratory course," *Biochem. Mol. Biol. Educ.*, vol. 43, no. 1, pp. 52–59, 2015.
- [16] J. Laverdant *et al.*, "Experimental Determination of the Fluorescence Quantum Yield of Semiconductor Nanocrystals," *Materials (Basel)*, vol. 4, no. 7, pp. 1182–1193, 2011.
- [17] N. B. D. Lima, S. M. C. Gonçalves, S. A. Júnior, and A. M. Simas, "A comprehensive strategy

- to boost the quantum yield of luminescence of europium complexes,” *Sci. Rep.*, vol. 3, no. Iii, pp. 1–8, 2013.
- [18] O. SHIMOMURA, F. H. JOHNSON, and Y. SAIGA, “Extraction, purification and properties of aequorin, a bioluminescent protein from the luminous hydromedusan, *Aequorea*,” *J. Cell. Comp. Physiol.*, vol. 59, no. 165, pp. 223–39, Jun. 1962.
 - [19] J. D. Pédelacq, S. Cabantous, T. Tran, T. C. Terwilliger, and G. S. Waldo, “Engineering and characterization of a superfolder green fluorescent protein,” *Nat. Biotechnol.*, vol. 24, no. 1, pp. 79–88, Jan. 2006.
 - [20] N. C. Shaner, P. A. Steinbach, and R. Y. Tsien, “A guide to choosing fluorescent proteins,” *Nat. Methods*, vol. 2, no. 12, pp. 905–909, Dec. 2005.
 - [21] B. P. Cormack, R. H. Valdivia, and S. Falkow, “FACS-optimized mutants of the green fluorescent protein (GFP),” *Gene*, vol. 173, no. 1 Spec No, pp. 33–8, 1996.
 - [22] T. Förster, “Zwischenmolekulare Energiewanderung und Fluoreszenz,” *Ann. Phys.*, vol. 437, no. 1–2, pp. 55–75, 1948.
 - *[23] E. A. Jares-Erijman and T. M. Jovin, “FRET imaging,” *Nature Biotechnology*, vol. 21, no. 11, pp. 1387–1395, Nov-2003.
 - *[24] S. Zadran, S. Standley, K. Wong, E. Otiniano, A. Amighi, and M. Baudry, “Fluorescence resonance energy transfer (FRET)-based biosensors: visualizing cellular dynamics and bioenergetics,” *Applied Microbiology and Biotechnology*, vol. 96, no. 4, pp. 895–902, 06-Nov-2012.
 - [25] B. OPELL, “Capture thread extensibility of orb-weaving spiders: testing punctuated and associative explanations of character evolution,” *Biol. J. Linn. Soc.*, vol. 70, no. 1, pp. 107–120, May 2000.
 - [26] K. M. Bonthron, F. Vollrath, B. K. Hunter, and J. K. M. Sanders, “The elasticity of spiders’ webs is due to water-induced mobility at a molecular level,” *Proc. R. Soc. B Biol. Sci.*, vol. 248, no. 1322, pp. 141–144, May 1992.
 - [27] N. Becker *et al.*, “Molecular nanosprings in spider capture-silk threads,” *Nat. Mater.*, vol. 2, no. 4, pp. 278–283, Apr. 2003.
 - [28] C. Grashoff *et al.*, “Measuring mechanical tension across vinculin reveals regulation of focal adhesion dynamics,” *Nature*, vol. 466, no. 7303, pp. 263–266, 2010.
 - [29] M. D. Brenner *et al.*, “Spider Silk Peptide Is a Compact, Linear Nanospring Ideal for Intracellular Tension Sensing,” *Nano Lett.*, vol. 16, no. 3, pp. 2096–2102, Mar. 2016.
 - [30] A. S. LaCroix, A. D. Lynch, M. E. Berginski, and B. D. Hoffman, “Tunable molecular tension sensors reveal extension-based control of vinculin loading,” *Elife*, vol. 7, pp. 1–36, Jul. 2018.
 - *[31] W. H. Ziegler, A. R. Gingras, D. R. Critchley, and J. Emsley, “Integrin connections to the cytoskeleton through talin and vinculin,” *Biochemical Society Transactions*, vol. 36, no. 2, pp. 235–239, 01-Apr-2008.
 - *[32] L. Science, “Attachment and Matrix Factors,” *BioFiles*, vol. 3, no. 8, pp. 1–28, 2008.
 - *[33] E. Ruoslahti, “RGD AND OTHER RECOGNITION SEQUENCES FOR INTEGRINS,” *Annual Review of Cell and Developmental Biology*, vol. 12, no. 1, pp. 697–715, Nov-1996.
 - [34] C. L. Gilchrist *et al.*, “TRPV4-mediated calcium signaling in mesenchymal stem cells regulates aligned collagen matrix formation and vinculin tension,” *Proc. Natl. Acad. Sci.*, vol. 116, no. 6, pp. 1992–1997, Feb. 2019.

- [35] F. Li *et al.*, “Vinculin Force Sensor Detects Tumor-Osteocyte Interactions,” *Sci. Rep.*, vol. 9, no. 1, p. 5615, Dec. 2019.
- [36] A. H. Huber and W. I. Weis, “The structure of the beta-catenin/E-cadherin complex and the molecular basis of diverse ligand recognition by beta-catenin,” *Cell*, vol. 105, no. 3, pp. 391–402, May 2001.
- [37] K. Tamura, W. S. Shan, W. A. Hendrickson, D. R. Colman, and L. Shapiro, “Structure-function analysis of cell adhesion by neural (N-) cadherin,” *Neuron*, vol. 20, no. 6, pp. 1153–1163, Jun. 1998.
- [38] D. E. Conway, M. T. Breckenridge, E. Hinde, E. Gratton, C. S. Chen, and M. A. Schwartz, “Fluid Shear Stress on Endothelial Cells Modulates Mechanical Tension across VE-Cadherin and PECAM-1,” *Curr. Biol.*, vol. 23, no. 11, pp. 1024–1030, Jun. 2013.
- [39] M. Saitoh, T. Ishikawa, S. Matsushima, M. Naka, and H. Hidaka, “Selective inhibition of catalytic activity of smooth muscle myosin light chain kinase,” *J. Biol. Chem.*, vol. 262, no. 16, pp. 7796–7801, 1987.
- [40] J. A. Cooper, “Effects of cytochalasin and phalloidin on actin,” *The Journal of Cell Biology*, vol. 105, no. 4, pp. 1473–1478, 01-Oct-1987.
- [41] D. Cai *et al.*, “Mechanical Feedback through E-Cadherin Promotes Direction Sensing during Collective Cell Migration,” *Cell*, vol. 157, no. 5, pp. 1146–1159, May 2014.
- [42] D. Eder, K. Basler, and C. M. Aegerter, “Challenging FRET-based E-Cadherin force measurements in *Drosophila*,” *Sci. Rep.*, vol. 7, no. 1, p. 13692, Dec. 2017.
- [43] C. Hahn and M. A. Schwartz, “Mechanotransduction in vascular physiology and atherogenesis,” *Nature Reviews Molecular Cell Biology*, vol. 10, no. 1, pp. 53–62, Jan-2009.
- *[44] M. D. Kottke, “The desmosome: cell science lessons from human diseases,” *Journal of Cell Science*, vol. 119, no. 5, pp. 797–806, 01-Mar-2006.
- *[45] D. R. Garrod, A. J. Merritt, and Z. Nie, “Desmosomal adhesion: structural basis, molecular mechanism and regulation (Review),” *Molecular Membrane Biology*, vol. 19, no. 2, pp. 81–94, 09-Jan-2002.
- *[46] Y. S.W., A. B., S. N., and A. A.R., “Blistering disorders: Diagnosis and treatment,” *Dermatologic Therapy*, vol. 16, no. 3, pp. 214–223, 2003.
- [47] S. Baddam *et al.*, “The Desmosomal Cadherin Desmoglein-2 Experiences Mechanical Tension as Demonstrated by a FRET-Based Tension Biosensor Expressed in Living Cells,” *Cells*, vol. 7, no. 7, p. 66, Jun. 2018.
- [48] A. J. Price, A.-L. Cost, H. Ungewiß, J. Waschke, A. R. Dunn, and C. Grashoff, “Mechanical loading of desmosomes depends on the magnitude and orientation of external stress,” *Nat. Commun.*, vol. 9, no. 1, p. 5284, 2018.
- [49] A. P. Kowalczyk *et al.*, “The amino-terminal domain of desmoplakin binds to plakoglobin and clusters desmosomal cadherin-plakoglobin complexes,” *J. Cell Biol.*, vol. 139, no. 3, pp. 773–784, Nov. 1997.
- [50] R. M. Cabral *et al.*, “The DSPII splice variant is crucial for desmosome-mediated adhesion in HaCaT keratinocytes,” *J. Cell Sci.*, vol. 125, no. 12, pp. 2853–2861, Jun. 2012.
- [51] W. Li *et al.*, “A Membrane-Bound Biosensor Visualizes Shear Stress-Induced Inhomogeneous Alteration of Cell Membrane Tension,” *iScience*, vol. 7, pp. 180–190, Sep. 2018.
- *[52] H. J. Green and N. H. Brown, “Integrin intracellular machinery in action,” *Experimental Cell Research*, vol. 378, no. 2, Elsevier Inc., pp. 226–231, May-2019.

- *[53] B. Klapholz and N. H. Brown, “Talin – the master of integrin adhesions,” *Journal of Cell Science*, vol. 130, no. 15, pp. 2435–2446, 01-Aug-2017.
- [54] R. O. McCann and S. W. Craig, “The I/LWEQ module: a conserved sequence that signifies F-actin binding in functionally diverse proteins from yeast to mammals,” *Proc. Natl. Acad. Sci.*, vol. 94, no. 11, pp. 5679–5684, May 2002.
- [55] M. D. Bass, B. J. Smith, S. A. Prigent, and D. R. Critchley, “Talin contains three similar vinculin-binding sites predicted to form an amphipathic helix,” *Biochem. J.*, vol. 341 (Pt 2, no. 2, pp. 257–63, Jul. 1999.
- [56] S. E. Lee, S. Chunsriviro, R. D. Kamm, and M. R. K. Mofrad, “Molecular Dynamics Study of Talin-Vinculin Binding,” *Biophys. J.*, vol. 95, no. 4, pp. 2027–2036, Aug. 2008.
- [57] A. Kumar *et al.*, “Talin tension sensor reveals novel features of focal adhesion force transmission and mechanosensitivity,” *J. Cell Biol.*, vol. 213, no. 3, pp. 371–383, May 2016.
- [58] A. F. Straight, “Dissecting Temporal and Spatial Control of Cytokinesis with a Myosin II Inhibitor,” *Science (80-.)*, vol. 299, no. 5613, pp. 1743–1747, Mar. 2003.
- [59] P. Hotulainen and P. Lappalainen, “Stress fibers are generated by two distinct actin assembly mechanisms in motile cells,” *J. Cell Biol.*, vol. 173, no. 3, pp. 383–394, May 2006.
- [60] R. E. Gough and B. T. Goult, “The tale of two talins - two isoforms to fine-tune integrin signalling,” *FEBS Lett.*, vol. 592, no. 12, pp. 2108–2125, Jun. 2018.
- [61] B. L. Blakely *et al.*, “A DNA-based molecular probe for optically reporting cellular traction forces,” *Nat. Methods*, vol. 11, no. 12, pp. 1229–1232, Dec. 2014.
- [62] K. Austen *et al.*, “Extracellular rigidity sensing by talin isoform-specific mechanical linkages,” *Nat. Cell Biol.*, vol. 17, no. 12, pp. 1597–1606, Dec. 2015.
- [63] G. Zoldak, J. Stigler, B. Pelz, H. Li, and M. Rief, “Ultrafast folding kinetics and cooperativity of villin headpiece in single-molecule force spectroscopy,” *Proc. Natl. Acad. Sci.*, vol. 110, no. 45, pp. 18156–18161, Nov. 2013.
- [64] A. Kumar, K. L. Anderson, M. F. Swift, D. Hanein, N. Volkmann, and M. A. Schwartz, “Local Tension on Talin in Focal Adhesions Correlates with F-Actin Alignment at the Nanometer Scale,” *Biophys. J.*, vol. 115, no. 8, pp. 1569–1579, Oct. 2018.
- [65] S. B. Lemke, T. Weidemann, A.-L. Cost, C. Grashoff, and F. Schnorrer, “A small proportion of Talin molecules transmit forces at developing muscle attachments in vivo,” *PLOS Biol.*, vol. 17, no. 3, p. e3000057, Mar. 2019.
- [66] P. Ringer *et al.*, “Multiplexing molecular tension sensors reveals piconewton force gradient across talin-1,” *Nat. Methods*, vol. 14, no. 11, pp. 1090–1096, 2017.